



Stress tunable microwave absorption of ferromagnetic microwires for sensing applications

Faxiang Qin^{a,b,*}, V.V.Popov^c, Hua-Xin Peng^a

^a Advanced Composite Center for Innovation and Science, Department of Aerospace Engineering, University of Bristol, University Walk, Bristol, BS8 1TR, UK

^b Lab-STICC, Université de Brest, CS 93837, 6 Avenue Le Gorgeu, 29238 Brest Cedex 3, France

^c Taurida National University, Simferopol, Ukraine

ARTICLE INFO

Article history:

Received 25 February 2011

Received in revised form 13 July 2011

Accepted 15 July 2011

Available online 22 July 2011

Keywords:

Low field absorption

Amorphous glass-coated microwires

Microwave

PACS:

75.50.Kj

76.50.+g

75.80.+q

ABSTRACT

In the present work, we have studied the low field absorption (LFA) at 9 GHz of a set of Co-based glass-coated microwires in the presence of tensile stresses along the wire axis. The results reveal that the absorption profiles bear valve-like features associated with microwave magnetoimpedance effect. The stress applied along the wire axis compensates the reverse effect of magnetic field on absorption. The peak shown in the derivative LFA spectra becomes wider with increasing stress and moves to higher field, corresponding to the magnetization process. A larger ratio of metal to total diameter was found to be favorable to microwave absorption due to the smaller anisotropy and also gave rise to a larger magnetostriction constant. The influences of stress/magnetic field on the absorption as well as the shift of feature stress with wire geometry were discussed in the context of an effective microwire-based sensor design. Calculations of magnetostriction constant by the derived field dependence of anisotropy field were also performed to demonstrate the usefulness of stress tunable microwave absorption characteristics as a research tool.

© 2011 Elsevier B.V. All rights reserved.

1. Introduction

Co-based amorphous glass-coated microwires (AGCMs) have a unique circular magnetic anisotropy due to coupling between the negative magnetostriction and frozen-in stress. Such anisotropy is important to realize a large and sensitive magnetoimpedance (MI) effect for applications in miniature magnetic sensors [1–3]. The MI effect refers to a strong variation in the high frequency impedance of a magnetic conductor subject to a small dc magnetic field, which is observed at frequencies when the skin effect is strong (i.e., skin depth is small). Based on the frequency range, it can be classified into three regions [4–6]: (i) at a relatively low-frequency range of a few hundred kHz to MHz, the change of impedance is mainly due to circular domain wall dynamics; (ii) at the intermediate frequency range from a few MHz to a few hundred MHz, the domain wall motion is strongly damped and the rotational processes mainly contribute to the ac permeability and impedance change; (iii) at frequencies of the GHz range where ferromagnetic resonance (FMR) occurs, the rotational permeability becomes less sensitive to the field and the impedance change is related to the

concomitant absorption occurred at low fields. It should be noted that MI differs essentially from FMR as the former is a classical electromagnetic phenomenon whilst the latter can be understood by quantum mechanics [7]. Yet when FMR happens, the absorption at low fields can also be observed, this low field absorption (LFA) is strongly correlated to MI. Both phenomena depend intimately on the magnetic anisotropy determined by the domain configuration [8].

The high-frequency absorption behavior of amorphous ferromagnetic materials, among others, is of considerable interest from the application point of view [9,10]. Amorphous magnetic microwires were initially advanced for absorption of electromagnetic radiation. Their intriguing high-frequency properties also make them very appealing for sensing elements, radiofrequency applications, etc. Valenzuela et al. [11] pointed out that increasing temperature encouraged the structural relaxation in Ni–Zn ferrite and consequently a gradually narrower peak in the LFA profiles was spotted. An abrupt change of linewidth occurred at Curie temperature whereby the electron paramagnetic resonance took place. Montiel et al. [12] elucidated the influence of microwire geometry on the microwave absorption behavior of CoFeBSi microwire. They found out that a lower metal-to-glass ratio was in favor of anisotropy field corresponding to a shift of absorption peak to higher field. Medina et al. [13] pinpointed the impact of magnetic field orientation on the absorption signal and demonstrated the

* Corresponding author at: Lab-STICC, Université de Brest, CS 93837, 6 Avenue Le Gorgeu, 29238 Brest Cedex 3, France.

E-mail addresses: faxiang.qin@bristol.ac.uk, faxiang.qin@gmail.com (F. Qin).

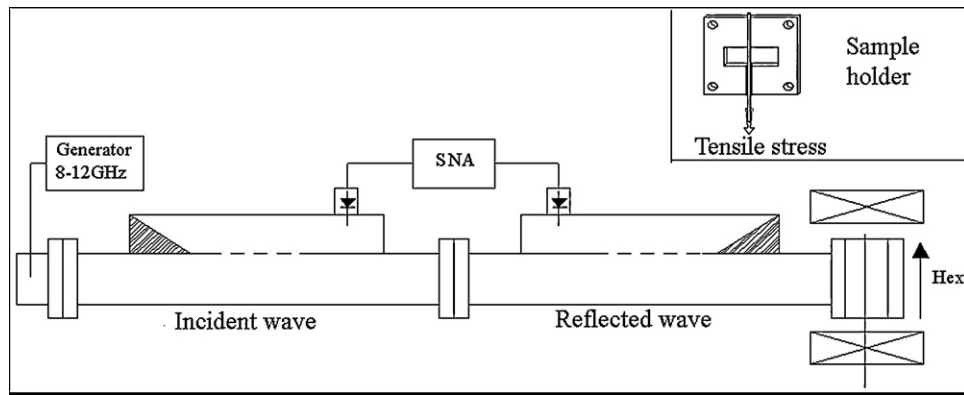


Fig. 1. Schematic diagram of the SNA assembly and the inset shows the mode of tensile stress application on the measured microwire.

Table 1

The geometrical parameters, absorption under zero magnetic field ($|A|_0$) and 7 Oe ($|A|$) measured at 9 GHz with applied stress of 300 MPa.

	d	t	p	$ A _0$, $ A $
Wire A	30.6	5.2	0.746	30%, 42%
Wire B	12.4	1.1	0.849	46%, 56%
Wire C	18.0	0.6	0.938	50%, 71%

positive effect of magnetic field along the easy axis of an amorphous ribbon. In another aspect, the role of stress on the GMI properties as well as stress-impedance effect have been extensively investigated (see, e.g. [14–16]). As the stress is critical in modifying the magnetoelastic behavior of microwires, it would be of strong interest to study the absorption features conditioned by the stress at gigahertz frequencies. The results obtained can serve as a guide for investigating the microwave properties of microwire composites of much interest.

In this context, we have conducted a study of stress tunable behavior at microwave frequency of a set of Co-based microwires at 9–10 GHz. The LFA spectra show a strong sensitivity of absorption to the applied stress.

2. Experimental

Soft magnetic amorphous glass-coated microwires of $\text{Co}_{67}\text{Fe}_{3.9}\text{Ni}_{1.4}\text{B}_{11.5}\text{Si}_{14.5}\text{Mo}_{1.7}$ with different geometrical parameters were fabricated by a modified Taylor–Ulitskiy method [17]. The metallic core diameter and the glass thickness of the microwires were measured by scanning electron microscopy (SEM). The geometrical parameters of the microwires (the metallic core diameter (d), the glass thickness (t), and the metal-to-total diameter ratio ($p=d/(d+2t)$) are summarized in Table 1. These microwires possess good soft magnetic properties owing to the nearly zero and negative magnetostriction ($\lambda \sim -10^{-7}$). The reflection loss was measured by transmission line method using a modified scalar network analyzer assembly (SNA) as schematically shown in Fig. 1. The studied wire with 1 cm excited length, which excludes the multi-mode resonances, was placed in front of metallic short and perpendicular to the geomagnetic field. The inset of Fig. 1 illustrates the way of applying tensile stress to the microwire within the sample holder. More details about the setup can be found elsewhere [18]. Note that in the present geometry, the reflection coefficient is not sensitive to the wire displacement.

3. Results

Fig. 2 depicts the field dependence of absorption of wire A at varied stresses ranging from 37 MPa to 1263 MPa. When stress is no more than 371 MPa, the absorption shows strong field dependence and the applied field increases the absorption till saturation in analogy to the valve-like GMI profiles [19]. At $\sigma = 743$ MPa, the single peak feature becomes obscured with the less influence of magnetic field. When applied stress reaches 1114 MPa and 1263 MPa the absorption becomes almost independent of magnetic field. At differing magnetic fields, the stress exerts different influence on

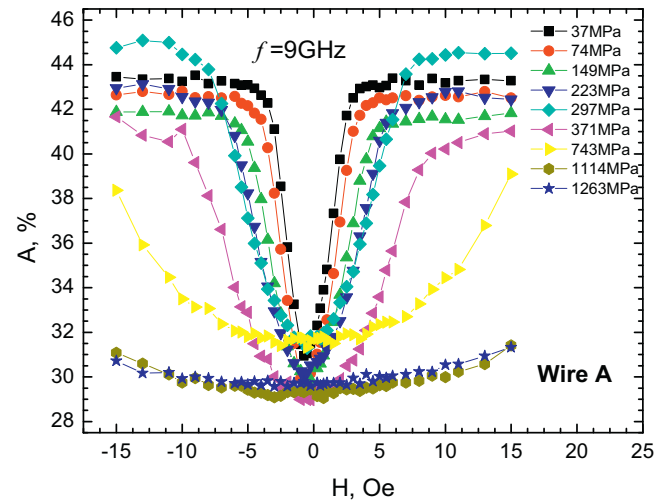


Fig. 2. Axial field dependence of absorption in presence of varying stress at 9 GHz for wire A.

the absorption. To better understand the impact of stress and magnetic field on the absorption, we plot Fig. 3 to show the stress dependence of absorption at four featured magnetic fields. Interestingly, at field as small as 0.75 Oe, the stress has an insignificant influence on the absorption. But with increasing field, the absorp-

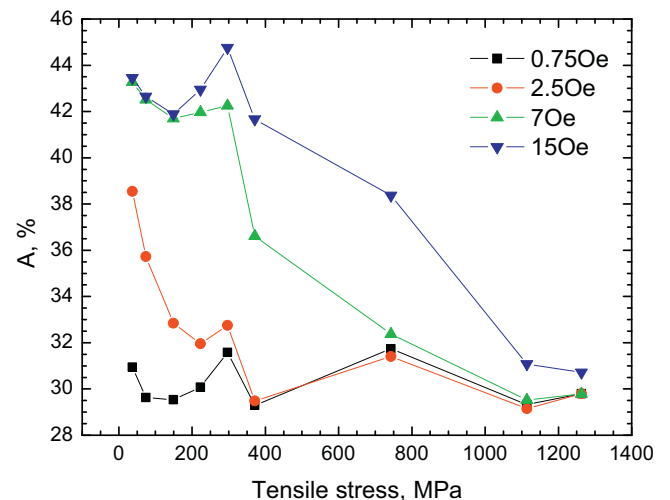


Fig. 3. Tensile stress dependence of absorption at varying magnetic fields for wire A.

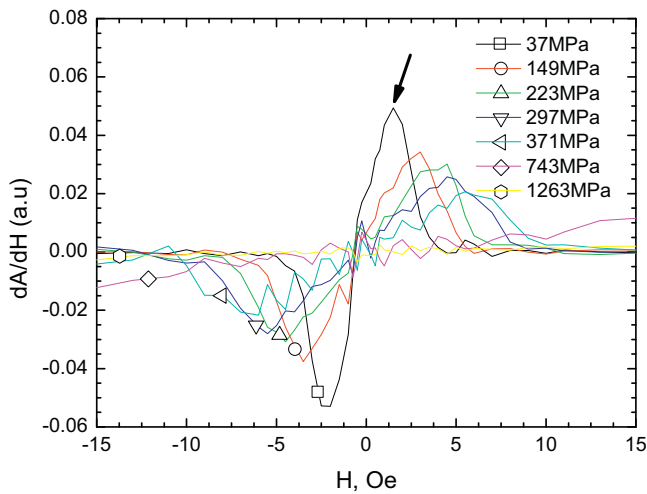


Fig. 4. Axial field dependence of derivative absorption in presence of varying stress at 9 GHz for wire A.

tion becomes more stress independent. A maximum absorption is observed for all curves at 297 MPa.

In the derivative absorption profiles (Fig. 4), the absorption peaks are found to become wider and shift to a higher magnetic field with increasing applied tensile stress. When the stress reaches 743 MPa, the peak is cancelled. As the peak-to-peak distance in an absorption curve is approximated twice the anisotropy field (H_k) [8], the anisotropy field is then derived as a function of stress as illustrated in Fig. 5. The fitting curve is performed with a second-order polynomial of the form $H_k = a\sigma^2 + b\sigma + c$, where a , b , c are constants.

The absorption spectra and corresponding derivative profiles of the other two wires (wire B and C) with different diameters are presented in Figs. 6 and 7. The absorption at zero magnetic field reaches 46% and 50%, respectively, which is around 20% larger than that of wire A. To clearly illustrate the influence of wire geometry on the absorption, we plot Fig. 8 to show the stress dependence of absorption at 7 Oe. The absorption increases with ratio of metal to total diameter p . Interestingly, the feature stress, where an abrupt increase of absorption occurs, is observed for all three wires and it shifts to higher value for wire C with $p = 0.938$. At c.a. 300 MPa, when comparing the absorption for $H = 7$ Oe with that for zero magnetic field, the absorption reduction for wire C is twice that of the other two wires, as given in Table 1.

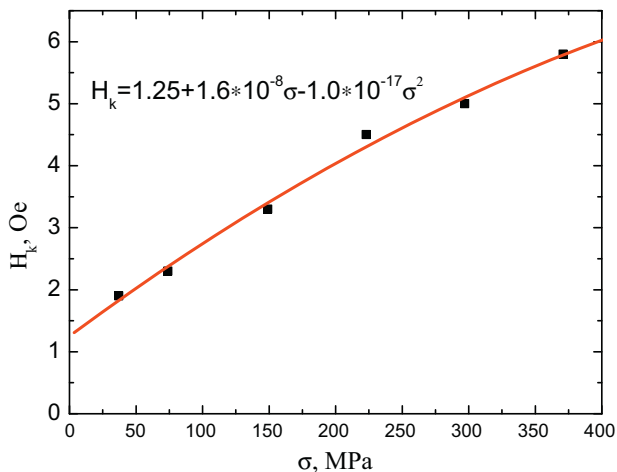


Fig. 5. Applied stress dependence of anisotropy field for wire A.

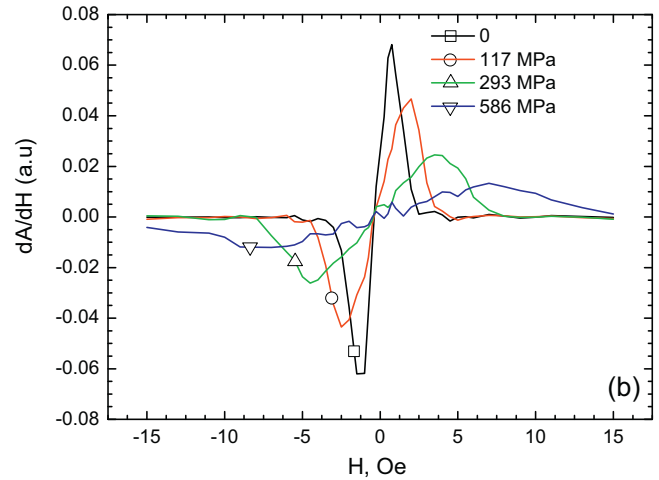
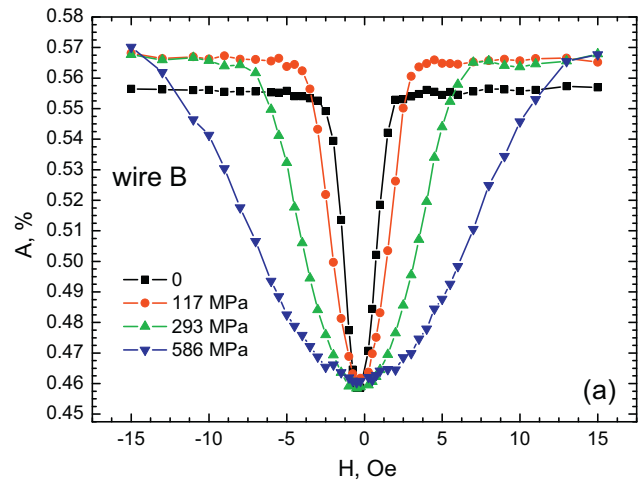


Fig. 6. Axial field dependence of absorption (a) and derivative absorption profiles (b) in the presence of varying stress at 9 GHz for wire B.

Fig. 9 summarizes the evolution of anisotropy field with stress for all three wires; curves are fitted in the same way as those in Fig. 5. The value of constant b is slightly decreased with increasing p , indicating a reduction of magnetostriction. The inset of Fig. 9 shows derived $H_k(p)$ relationship at 300 MPa. The anisotropy field is also decreased with increasing p .

4. Discussion

4.1. Low field absorption of the microwire

The absorption constant of the microwire, by definition can be expressed as the reciprocal of skin depth associated with electrical resistivity (ρ), circumferential magnetic permeability (μ) and frequency (f) via the following formula [20]:

$$\alpha = \frac{1}{\delta} = \sqrt{\frac{\pi f \mu}{\rho}} \quad (1)$$

where μ is dependent on the susceptibility (χ) and the angle (θ) between magnetization vector and the wire axis, formulated as [19]:

$$\mu = 1 + 4\pi \cos^2(\theta) \chi \quad (2)$$

The application of magnetic field along the wire axis increases the circumferential magnetic permeability by rotating the magnetization vector towards the wire axis and hence the absorption constant as the external field is below anisotropy field. On the other

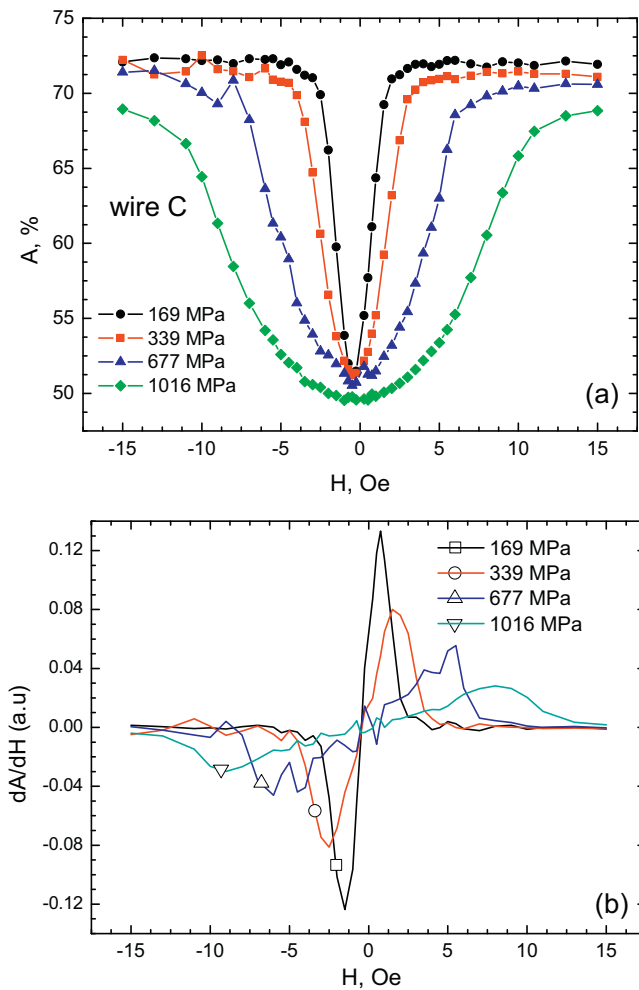


Fig. 7. Axial field dependence of absorption (a) and derivative absorption profiles (b) in the presence of varying stress at 9 GHz for wire C.

hand, when a stress is applied along the microwires with a negative magnetostriction, the magnetization vector rotates away from the axis direction when possible. As a result, the circumferential magnetic permeability is decreased and hence the absorption is reduced according to Eq. (1) [14]. It is expected, therefore, that

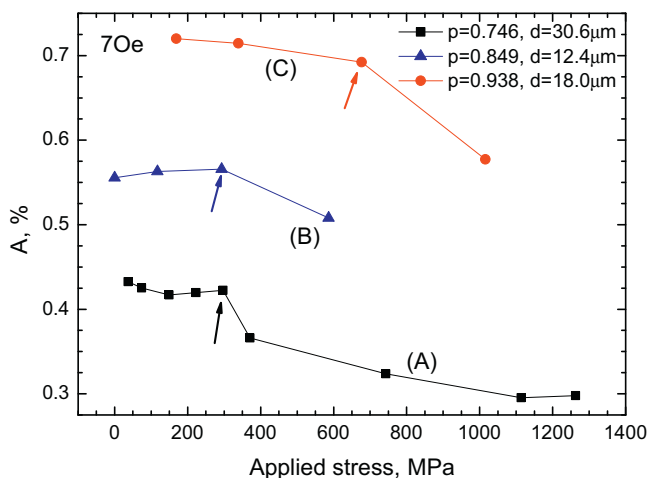


Fig. 8. Stress dependence of absorption for three wires with different geometry. The arrows indicate the feature stress for three samples, respectively.

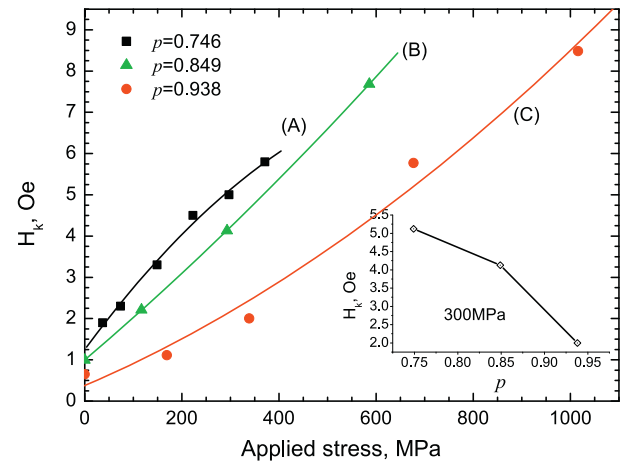


Fig. 9. Stress dependence of anisotropy field H_k for three wires with different geometry. The inset shows p dependence of H_k at 300 MPa.

the application of longitudinal stress will compensate the effect of the magnetic field. This is evidenced by Fig. 3. The influence of stress is more obvious with the increasing magnetic field. The maximum applied stress of 1263 MPa encourages the absorption back to the original value by offsetting the effects of magnetic field. The magnetic field along the wire axis is desirable for the absorption of microwires and can also be utilized to increase the stress sensitivity of absorption. Upon analyzing the data in Fig. 3, it can be obtained the sensitivity of absorption to stress (the ratio of the variation of absorption to that of corresponding stress) increases by c.a. 39 times when the field increases from 0.75 to 15 Oe. This is of great significance in designing wire-based stress sensor.

The derivative profiles of low field absorption (Fig. 4) afford us a compelling revelation of the stress impact on the absorption, as the shape of the peak is correlated to the magnetization process [11]. The field where the peak occurs can then be estimated as anisotropy field. That the peak (as indicated by the arrow in Fig. 4) becomes wider and shifts to higher field with stress indicates the reduction of soft magnetic property and hence the circumferential permeability, which again confirms the relationship between longitudinal stress and absorption as discussed above. Note that when $\sigma \geq 743$ MPa, the magnetoelastic behavior of the microwires are profoundly modified, and the absorption and anisotropy field tend to be independent of applied magnetic field. This indicates a saturation of longitudinal impedance due to the excessive stress. This is very illuminating when it comes to the sensor design. Specifically, the service condition in terms of the external stress has to be accounted when the microwire is designed for a field sensor.

The usefulness of low field absorption as an effective research tool is demonstrated in Fig. 5. Using the fitted equation, we can calculate the magnetostriction constant [21]. As $\lambda_s = -(\mu_0 M_s / 3)(dH_k / d\sigma)$, we can then obtain $\lambda_s = -(\mu_0 M_s / 3)(2a\sigma + b)$. Thus, the unstressed value of the magnetostriction, denoted as $\lambda_{s,0}$, can be given by $\lambda_{s,0} = -(\mu_0 M_s / 3)b$. Following these calculations, we have determined $\lambda_{s,0} = -2.8 \times 10^{-7}$. In addition to being a tool to estimate the magnetostriction constant, it can also serve as a probe into the magnetization mechanism of the microwires. Therefore, the absorption can be instrumental to a host of relevant magnetic studies.

4.2. Effects of metal-to-total diameter ratio on LFA

Let us first recall that the Co-based microwire consists of inner core with axial anisotropy and outer shell with circular anisotropy

in terms of domain structure [4]. As proposed by Antonov et al., the magnetic properties are determined by the magnetoelastic interactions, which are mainly governed by the frozen-in stress induced during fabrication process. The anisotropy field can be determined by the following equation [22]:

$$H_k = \frac{3\lambda_s}{M_s} \left(\sigma_{zz} - \sigma_{\phi\phi} + \frac{1}{(1-k)p^2 + k\bar{\sigma}} \right), \quad (3)$$

where σ_{zz} , $\sigma_{\phi\phi}$ represent the residual stress component in the axial and azimuthal direction, respectively; $\bar{\sigma}_{zz}$ denotes the average applied axial stress. k is the metal-to-glass ratio of Young's moduli. As the difference between σ_{zz} and $\sigma_{\phi\phi}$ decreases with decreasing p and the Young's modulus of metallic core is almost twice that of glass coat, the anisotropy field therefore decreases with increasing p . In addition, increasing p would also give rise to a decreased anisotropy angle (the angle between the magnetization easy axis and the wire axis) due to the reduced internal stress. Thus, the absorption is improved with increasing p . This is fully consistent with our previous reports on the effect of metal-to-diameter ratio on GMI [23].

The shift of feature stress for wire C (Fig. 8) can also be explained by the relatively ill-defined anisotropy owing to the very large p . A much larger stress proves to be necessary to induce the change of anisotropy and hence the absorption. Likewise, a larger field sensitivity of absorption for wire C can be attributed to the fact that the magnitude of the anisotropy field determines that of the external field needed for driving the magnetization vector rotating towards the longitudinal axis, which is desirable for absorption.

The magnetostriction constant is generally decreased with the stress, according to $\lambda_s = \lambda_{s,0} - A\sigma$ [24,25], where $\lambda_{s,0}$ is the saturation magnetization at zero tensile stress. A is a positive coefficient susceptible to thermal treatments. $\lambda_{s,0}$ should be the same for all three wires with the same composition. But using the same method as did for wire A, one can determine the magnetostriction constant, -1.8×10^{-7} and -0.9×10^{-7} for wire B and C, respectively. This can be attributed to the fact that more residual stress is introduced during the fabrication process with decreasing p [23] and thereby reduced the magnetostriction constant to a relatively larger extent. All these results suggest the significance of wire geometry on the absorption and related properties. The principles generalized herein can be exploited for an optimized design of wire-based sensors. In order for an effective stress/field sensing in certain stress/field range, for instance, the wire geometry should be carefully evaluated and selected in terms of the behaviors discussed above.

5. Conclusions

The stress influence of low field absorption behavior at 9 GHz has been thoroughly discussed. It is shown that the peak in the derivative LFA profiles becomes wider and shifts to a higher field with increasing applied tensile stress along the wire axis, indicat-

ing a reduced soft magnetic property. The stress tunable LFA spectra have been adopted to measure the magnetostriction constant via the derived stress dependence of anisotropy field. A larger ratio of metal to total diameter is found to benefit microwave absorption due to the decrease of anisotropy and also gives rise to a larger magnetostriction constant. The shift of feature stress corresponding to an abrupt change of absorption with the wire geometry offers a guide for an optimized wire-based sensor design.

Acknowledgements

FXQ was supported through Overseas Research Students Awards Scheme and University of Bristol Postgraduate Student Scholarship. He would also like to acknowledge the current financial support provided by Conseil général du Finistère, France.

References

- [1] L.V. Panina, J. Magn. Magn. Mater. 249 (2002) 278–287.
- [2] C. García, V. Zhukova, M. Ipatov, J. González, J.M. Blanco, A. Zhukov, J. Alloys Compd. 488 (2009) 9–12.
- [3] C. García, V. Zhukova, J. González, A. Chizhik, J.M. Blanco, M. Ipatov, A. Zhukov, J. Alloys Compd. 488 (2009) 5–8.
- [4] M.H. Phan, H.X. Peng, Prog. Mater. Sci. 53 (2008) 323–420.
- [5] A. Yelon, D. Menard, M. Britel, P. Ciureanu, Appl. Phys. Lett. 69 (1996) 3084–3085.
- [6] M. Knobel, M. Vazquez, L. Kraus, in: K.H. Buschow (Ed.), Giant Magnetoimpedance, 2003.
- [7] R. Valenzuela, R. Zamorano, G. Alvarez, M.P. Gutiérrez, H. Montiel, J. Non Cryst. Solids 353 (2007) 768–772.
- [8] H. Montiel, G. Alvarez, I. Betancourt, R. Zamorano, R. Valenzuela, Appl. Phys. Lett. 86 (2005) 072503.
- [9] M. Vázquez, A.L. Adenot-Engelvin, J. Magn. Magn. Mater. 321 (2009) 2066–2073.
- [10] M. Vázquez, G. Badidni-Confalonieri, J. Torrejón, R. Valenzuela, H. Montiel, G. Alvarez, Third International Conference on Quantum, Nano and Micro Technologies, 2009.
- [11] R. Valenzuela, G. Alvarez, H. Montiel, M.P. Gutierrez, M.E. Mata-Zamora, F. Barron, J. Magn. Magn. Mater. 320 (2008) 1961–1965.
- [12] H. Montiel, G. Alvarez, M.P. Gutierrez, R. Zamorano, R. Valenzuela, IEEE Trans. Magn. 42 (2006) 3380–3382.
- [13] A.N. Medina, M. Knobel, S. Salem-Sugui, F.G. Gandra, J. Appl. Phys. 79 (1996) 5462–5464.
- [14] L.V. Panina, S.I. Sandacci, D.P. Makhnovskiy, J. Appl. Phys. 97 (2005) 013701–013706.
- [15] A. Zhukov, Adv. Funct. Mater. 16 (2006) 675–680.
- [16] C. García, A. Zhukov, V. Zhukova, M. Ipatov, J.M. Blanco, J. Gonzalez, IEEE Trans. Magn. 41 (2005) 3688–3690.
- [17] V.S. Larin, A.V. Torcunov, A. Zhukov, J. Gonzalez, M. Vazquez, L. Panina, J. Magn. Magn. Mater. 249 (2002) 39–45.
- [18] V.N. Berzhansky, V.I. Ponomarenko, V.V. Popov, A.V. Torkunov, Tech. Phys. Lett. 31 (2005) 959–960.
- [19] S.I. Sandacci, D.P. Makhnovskiy, L.V. Panina, J. Magn. Magn. Mater. 272–276 (2004) 1855–1857.
- [20] D.D.L. Chung, Carbon 39 (2001) 279–285.
- [21] M. Knobel, C. Gomez-Polo, M. Vazquez, J. Magn. Magn. Mater. 160 (1996) 243–244.
- [22] A.S. Antonov, et al., J. Phys. D: Appl. Phys. 32 (1999) 1788.
- [23] F.X. Qin, H.X. Peng, M.H. Phan, Solid State Commun. 150 (2010) 114–117.
- [24] A. Zhukov, V. Zhukova, J.M. Blanco, A.F. Cobeno, M. Vazquez, J. Gonzalez, J. Magn. Magn. Mater. 258–259 (2003) 151–157.
- [25] J.M. Blanco, P.G. Barbon, J. Gonzalez, C. Gomez-Polo, M. Vazquez, J. Magn. Magn. Mater. 104–107 (1992) 137–138.